Macroscopic Network Loading of Microscopic Travel Demand

Gunnar Flötteröd *

January 15, 2009

Report TRANSP-OR 090115
Transport and Mobility Laboratory
Ecole Polytechnique Fédérale de Lausanne
transp-or.epfl.ch

*Transp-OR, Ecole Polytechnique Fédérale de Lausanne, CH-1015 Lausanne, Switzerland, gunnar.floetteroed@epfl.ch

Abstract

This article presents a computationally efficient technique for the macroscopic (equation–based) network loading of microscopic (simulation–based) travel demand. It combines the expressive power of microsimulations as sampling tools for highly heterogeneous demand segments with mathematically well–understood macroscopic network loading procedures. The presented experimental results demonstrate the efficiency and precision of the approach even for large and complex scenarios. This work is intended to contribute to the understanding and application of microsimulation techniques in the context of mathematically motivated dynamic traffic assignment procedures.

Keywords: dynamic traffic assignment, demand microsimulation, network loading, traffic flow modeling

1 Introduction

Informally, the dynamic traffic assignment (DTA) problem is to attain consistency between a dynamic model of travel demand and a dynamic model of network supply. The feasibility of this problem, e.g., in terms of solution existence and uniqueness, depends on the mathematical properties of the involved model components. However, there also are computational issues, e.g., speed of convergence and required computer resources, that are just as relevant from an application point of view. Overall, the DTA problem requires computationally strong solution procedures for realistic models of convenient mathematical structure. This article investigates one aspect of this problem in that it proposes a simulation technique that efficiently links the subsequently described classes of demand and supply models.

Regarding the demand model, it is a well-recognized fact that the negligence of heterogeneity in the population by an overly aggregated model can cause severe biases (Ben-Akiva & Lerman, 1985). This observation led to the development of increasingly disaggregate demand models, the most extreme case of which are approaches where every traveler is modeled individually (Raney & Nagel, 2006). Because of their mathematical complexity, such models are typically evaluated through (micro)simulation (Train, 2003; Vovsha et al., 2004). This article assumes a microsimulation-based demand representation.

On the supply side, there exists a broad range of modeling approaches. Microscopic models describe the progression of individual vehicles through the network, whereas macroscopic models capture traffic flows at an aggregate level and describe the movement of continuous traffic streams through the system (Hoogendoorn & Bovy, 2001). While the former certainly bear the potential for arbitrarily detailed modeling, the latter have the important advantage of possessing well-understood mathematical features that strongly support the design of algorithms not only for the equilibration of demand and supply but also for, e.g., calibration and optimization. This article assumes a macroscopic supply model.

DTA requires to somehow feed the disaggregate demand into the aggre-

gate supply model. Traditionally, heterogeneous demand segments are captured by splitting traffic volumes into partial flows (commodities) (Hilliges & Weidlich, 1995; Kotsialos et al., 2002; Lebacque, 1996). For example, destination-bound commodities would exhibit different turning behavior at intersections in order to reach their destinations. However, the applicability of this approach to systems of realistic network size and demand heterogeneity is limited by the computational cost of tracking partial flows for every commodity on basically every link in the network. In microsimulation-based DTA, this difficulty is circumvented by loading individual trip-makers, which are sampled from the underlying commodity distribution, on the network (Ben-Akiva et al., 1998; Cetin et al., 2003; De Palma & Marchal, 2002; Mahmassani, 2001; Nökel & Schmidt, 2002). Two problems arise in this approach. First, the results are inherently stochastic. Second, the network loading procedure is of a simulation-based nature with only few guarantees regarding its mathematical properties (Peeta & Mahmassani, 1995).

This work combines the computational efficiency and expressive power of demand microsimulations with the mathematical convenience of equation-based supply models. The commodities are represented by massless particles (commodity samples) that are dispersed in the macroscopic flow. They drift along with the flow according to its spatiotemporal velocity field, and they guide the flow towards consistency with their individual-level driving choices. Commodity information for any spatiotemporal segment of the network can be recovered by counting the according particles within that segment. Despite of the microscopic demand representation, tractable equations are available for the evolution of the macroscopic network conditions. The particle discretization noise can be efficiently suppressed. The method is easy to implement in conjunction with broad classes of demand and supply models.

The remainder of this article is organized as follows. Section 2 specifies the proposed simulation approach. Section 3 investigates some of its theoretical properties, and Section 4 demonstrates its precision and computational feasibility for a large-scale application. Finally, the article is summarized in Section 5, and several applications of the method are indicated.

2 Specification

The proposed simulation technique can be applied to a variety of demand and supply models. Here, a general description is given that adopts specific modeling assumptions only where greater generality would introduce an unjustified notational overhead.

2.1 Microscopic demand model

For the sake generality, only the most disaggregate demand representation where every traveler is modeled as an individual entity is considered. The activity and traveling intentions of a simulated traveler are denoted as its plan. Physically, a plan describes a round trip through the transportation network, which comprises a sequence of trips that connect intermediate stops during which activities are conducted, including all associated timing information. The first and last activity of a plan typically take place at the traveler's home location.

Dynamic origin/destination (OD) matrices result naturally as aggregations of a traveler population's plan set. Vice versa, a given OD matrix can be represented in disaggregate terms if every trip contained in the OD matrix is associated with a single synthetic traveler the plan of which consists of that trip only. Beyond these transformations from and to OD matrices, the potential to account for more complex demand patterns renders the plan–based, individual–level demand representation applicable to all kinds of activity-based travel demand models (Bowman & Ben-Akiva, 1998).

2.2 Macroscopic supply model

The macroscopic traffic flow model representing the network supply is required little more than to specify a spatiotemporal velocity field on all links in the network. A discrete version of this model is assumed here because of its arguably greatest operational relevance; the subsequent developments

can be applied symmetrically in continuous conditions. The supply model is formalized in terms of a state space representation

$$\begin{aligned} \mathbf{x}^s(0) &= \mathbf{x}_0^s \\ \mathbf{x}^s(k+1) &= \mathbf{f}^s[\mathbf{x}^s(k), \boldsymbol{\beta}(k), k] \end{aligned} \tag{1}$$

where the vector $\mathbf{x}^s(k)$ denotes the supply model's state at discrete simulation time step k. For a spatially discretized 1st order model (such as the cell-transmission model (Daganzo, 1994; Daganzo, 1995)), this vector contains one element for every cell (homogeneous link segment) in the network. The single-commodity flow splits $\boldsymbol{\beta}(k) = (\beta_{ij}(k))$ from every upstream cell i to every downstream cell j at all intersections are exogenously specified. This notation comprises demand entries and exits if additional turning moves into the network and out of the network are allowed for. The vector-valued transition function $\mathbf{f}^s$ defines the system's evolution through time. It fully encapsulates the specifically chosen traffic flow model.

2.3 Particle movement

Consider a set of particles $n = 1 \ldots N$ that are floating through the network. Particles have no "mass" insofar as they do not contribute to the macroscopic occupancy in a cell. At the time of a particle's entrance into the network, an appropriate amount of macroscopic flow is also dismissed into the system, resulting in a mass balance between particles and total macroscopic occupancy.

The macroscopic traffic flow model specifies a local velocity $v_i(k)$ for all cells i in all time steps k. In every time step of duration T, each particle advances according to the local velocity in its current cell. Particle locations within a cell are continuous quantities, and their movement is regarded as continuous in time as well: When a particle crosses a cell boundary during a single move of duration T, it can freely choose its next cell according to its internal plan (if there is more than one downstream cell) and continue with the velocity encountered there until its available move time ends. This procedure is illustrated in Figure 1. The particle evaluates all traversed cells' velocities

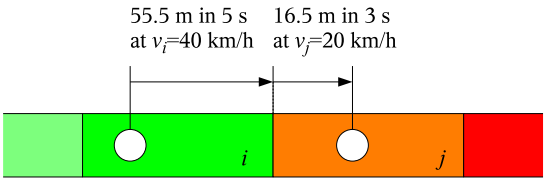

Figure 1: Particle movement across cell boundaries

A particle approaches the upstream end of a congested road segment. The time step duration is $T = 8\,s$. The particle needs $5\,s$ to reach the end of cell i at $v_i = 40$ km/h. During the remaining $3\,s$, it advances another $16.5\,m$ in cell j at $v_j = 20\,km/h$.

at the start time of its move. In consequence, this simulation scheme is imprecise in the order of a time step length, just as the macroscopic traffic flow model itself.

When a particle reaches its destination, it is removed from the system and an appropriate amount of macroscopic flow is also filtered out of the traffic stream passing the exit location.

2.4 Particle route choice

Having stated the influence of macroscopic dynamics on individual particles, the converse problem of synchronizing macroscopic flows with individual particle behavior is considered next.

The route choice of particle n is expressed by a vector $\mathbf{u}_n(k) = (u_{ij,n}(k))$ of turning move indicators

$$u_{ij,n}(k) = \begin{cases} 1 & \text{if } n \text{ proceeds from cell } i \text{ to } j \text{ at time step } k \\ 0 & \text{otherwise.} \end{cases} \tag{2}$$

This representation can account for network entries and exits through additional entry and exit cells that are located outside of the network (Cayford et al., 1997).

A demand state vector $\mathbf{x}^d(k) = (x_{ij}(k))$ is introduced. As a preliminary definition, let each element $x_{ij}(k)$ represent the average number of particles having turned from cell i into cell j until time step k:

$$\mathbf{x}^d(k) = \frac{1}{k+1} \sum_{k'=0}^{k} \sum_{n=1}^{N} \mathbf{u}_n(k'). \tag{3}$$

Equivalently,

$$\mathbf{x}^d(k) = \frac{k}{k+1} \mathbf{x}^d(k-1) + \frac{1}{k+1} \sum_{n=1}^{N} \mathbf{u}_n(k) \tag{4}$$

for $k = 0, 1, \ldots$ with $\mathbf{x}^d(-1) = 0$. The macroscopic turning fractions $\boldsymbol{\beta}(k) = (\beta_{ij}(k))$ used in (1) are now specified as functions $\boldsymbol{\beta}(\mathbf{x}^d(k)) = (\beta_{ij}(\mathbf{x}^d(k)))$ of the turning counters where

$$\beta_{ij}(\mathbf{x}^d(k)) = \frac{x_{ij}(k)}{\sum_l x_{il}(k)}. \tag{5}$$

This is a maximum likelihood estimator of the microscopic turning probabilities if the particle turning moves follows a stationary multinomial distribution (Jones & Vines, 1998). The resulting estimates can be directly fed into the macroscopic traffic flow model by a substitution of $\boldsymbol{\beta}$ in (1). In order to avoid undefined $0/0$ divisions at the beginning of a simulation, the turning counters should be initialized with small positive values instead of all zeros.

Specification (4) works well only for stationary turning probabilities. In the following, two possibilities to account for time-dependency in these probabilities are discussed. To begin with, consider the naive approach

$$\mathbf{x}^d(k) = \sum_{n=1}^{N} \mathbf{u}_n(k). \tag{6}$$

It does not exhibit the infinite memory of (4), thus it immediately tracks all demand dynamics, but it fails for low flow rates and short time step lengths because of the frequent occurrence of $0/0$ divisions in (5).

To milden this problem, a rectangular probability distribution of the location of a vehicle may be assumed. This can be realized by assigning one particle to the front of this distribution and a second particle to its end, with the corresponding macroscopic flow being dismissed into the network such that it is located between the particles. Denoting the turning move indicator of vehicle n's second particle by $\mathbf{v}_n(k)$, one obtains

$$\mathbf{x}^d(k) = \frac{1}{K}\sum_{n=1}^{N}(\mathbf{u}_n(k) - \mathbf{v}_n(k)) \tag{7}$$

where K is the average number of time steps a vehicle distribution needs to cross an intersection.

A computationally more efficient approach that disposes of the second particle is to assume that the time step of a vehicle's arrival at an intersection is geometrically distributed and that the actual particle identifies the first possible time of arrival. This results in the turning counter update equation

$$\mathbf{x}^d(k) = w\mathbf{x}^d(k-1) + (1-w)\sum_{n=1}^{N}\mathbf{u}_n(k) \tag{8}$$

where $w \in (0,1)$ specifies the width of the arrival distribution. A convenient property of this filter is its infinite memory: Even if no particles reach an intersection for a while, the turning counters remain strictly positive and thus ensure well-defined flow splits in (5).

A unified state space representation of this system can be given. Let

$$\mathbf{x}(k) = \begin{bmatrix} \mathbf{x}^s(k) \\ \mathbf{x}^d(k) \end{bmatrix} \tag{9}$$

and

$$\mathbf{f}[\mathbf{x}(k), \mathbf{u}_1(k) \dots \mathbf{u}_N(k), k] = \begin{bmatrix} \mathbf{f}^s[\mathbf{x}^s(k), \boldsymbol{\beta}(\mathbf{x}^d(k)), k] \\ \mathbf{f}^d[\mathbf{x}^d(k), \mathbf{u}_1(k) \dots \mathbf{u}_N(k), k] \end{bmatrix} \tag{10}$$

where $\mathbf{f}^d$ is, e.g, (7) or (8). This results in

$$\mathbf{x}(k+1) = \mathbf{f}[\mathbf{x}(k), \mathbf{u}_1(k) \dots \mathbf{u}_N(k), k]. \tag{11}$$

According to the notational conventions of control theory, the turning move indicators $\mathbf{u}_n$ act as control variables in this model, and, in fact, the individual particle behavior steers the macroscopic traffic flow. Note that $\mathbf{x}$ does not account for the microscopic states of individual particles, which could, however, be formalized along these lines, if needed. (For example, the rectangular vehicle distribution assumed in (7) requires that the second particle memorizes and imitates the turning moves of the leading one.)

The purpose of (11) is to demonstrate that the macroscopic network loading of a microscopic demand results in a mathematically tractable representation of the macroscopic network conditions. For example, if the traffic flow model is differentiable with respect to the turning fractions, (11) allows to linearly predict the effect of individual-level behavior on the global network conditions. Section 5 indicates some applications that exploit this property.

3 Theoretical investigation

The proposed simulation technique is analyzed in stationary conditions without network entries and exits such that the expected stationary flow μ_j through link j becomes a linear combination of its upstream flows:

$$\mu_j = \sum_{ij} p_{ij}\mu_i \tag{12}$$

where p_{ij} is the true turning probability from link i to link j in the particle population.

Denote by q_i the microscopic flow through link i, by μ_i its expectation, by σ_i^2 its variance, and by q_{ij} the microscopic flow from link i to link j. In order to obtain the variance $\mathrm{VAR}\{q_{ij}\}$, the identity

$$\mathrm{VAR}\{q_{ij}\} = \mathrm{E}\{\mathrm{VAR}\{q_{ij} \mid q_i\}\} + \mathrm{VAR}\{\mathrm{E}\{q_{ij} \mid q_i\}\} \tag{13}$$

is used. Assuming independent turning decisions and hence a multinomial turning move distribution, this turns into

$$\begin{aligned} \mathrm{VAR}\{q_{ij}\} &= \mathrm{E}\{p_{ij}(1-p_{ij})q_i\} + \mathrm{VAR}\{p_{ij}q_i\} \\ &= p_{ij}(1-p_{ij})\mu_i + p_{ij}^2\sigma_i^2. \end{aligned} \tag{14}$$

If the intersection inflows are stochastically independent, this yields

$$\sigma_j^2 = \sum_i p_{ij}^2 \sigma_i^2 + \sum_i p_{ij}(1 - p_{ij})\mu_i. \tag{15}$$

The first sum on the right-hand side represents the propagation of the upstream flow variances through the intersection into link j. The second term constitutes an excitation that results from the variability of the particles' turning choices at the intersection.

All turning count filters (4), (6), (7), and (8) are unbiased in that $E\{x_{ij}\} = p_{ij}\mu_i$, where x_{ij} is the filtered turning count from link i to link j. A combination of (14) with the stationary transfer behavior of the respective filter yields

$$\mathrm{VAR}\{x_{ij}\} = \frac{p_{ij}(1 - p_{ij})}{C}\mu_i + \frac{p_{ij}^2}{C}\sigma_i^2 \tag{16}$$

where

$$C = \begin{cases} \infty & \text{infinite memory (4)} \\ 1 & \text{naive approach (6)} \\ K & \text{rectangular vehicle distr. (7) of temporal width } K \\ \frac{1+w}{1-w} & \text{geometrical arrival distr. (8) of temporal width } w. \end{cases} \tag{17}$$

Denote by $\tilde{q}_i$ the macroscopic flow through link i and by $\tilde{\sigma}_i^2$ its variance. An approximation of

$$\tilde{\sigma}_j^2 = \mathrm{VAR}\left\{\sum_i \beta_{ij}\tilde{q}_i\right\} = \mathrm{VAR}\left\{\sum_i \frac{x_{ij}}{\sum_l x_{il}}\tilde{q}_i\right\}$$

can be obtained (Goodman, 1962; Mood et al., 1974), but the result is somewhat unwieldy. Therefore, only the (reasonable) case of a large C is considered, which results in $\mathrm{VAR}\{x_{ij}\} \to 0$, almost deterministic flow splits $\beta_{ij} \to p_{ij}$, and, again for stochastically independent inflows, the simple approximation

$$\tilde{\sigma}_j^2 \approx \sum_i p_{ij}^2 \tilde{\sigma}_i^2. \tag{18}$$

This corresponds to the microscopic variance (15) without the excitation term that is due to the microscopic turning decisions – an intuitive result.

Only the transport of existing flow variance through the network remains. In a macroscopic setting, this variance can be further reduced by inserting the flows consistently with the assumed vehicle distributions: the wider these distributions, the smoother the flows and the lower the variance of the macroscopic network conditions. In addition, the dispersiveness of many spatiotemporally discretized network loading procedures contributes to this smoothing (Lebacque, 1996; LeVeque, 1992).

The overall message of this analysis is that the (typically undesirable) noise in the macroscopic network conditions that is injected through the microscopic particle simulation can be reduced to an arbitrary low degree by choosing sufficiently wide vehicle distributions and, consequently, a sufficiently inert turning counter update logic. However, the need to track dynamic turning probabilities imposes a limit on this inertia. The next section shows experimentally that a reasonable balance between noise reduction and tracking of time-dependent turning probabilities can be realized.

4 Experimental investigation

The precision and the computational feasibility of the proposed simulation technique are investigated. A detailed description of the experimental setting and all involved model components can be found in (Flötteröd, 2008).

The considered test case is modeled after the road network of Greater Berlin, which is illustrated in Figure 2. This network consists of 1 083 nodes and 2 459 unidirectional links. A synthetic population of 206 353 motorist travelers with complete daily plans is available for this network (Rieser et al., 2007). This is a 10 percent sample of Berlin's true motorist population. Thus, 10 macroscopic vehicle units need to be inserted together with one particle into the simulation. However, since the simulations are run on a thinned out version of the full Berlin network, the use of 2 instead of 10 macroscopic vehicle units per particle already creates realistic congestion patterns. An extended cell-transmission model is used as the network loading procedure.

Figure 2: Major road network of Greater Berlin

The network consists of 1 083 nodes and 2 459 unidirectional links. The two clippings indicate a locally high modeling resolution.

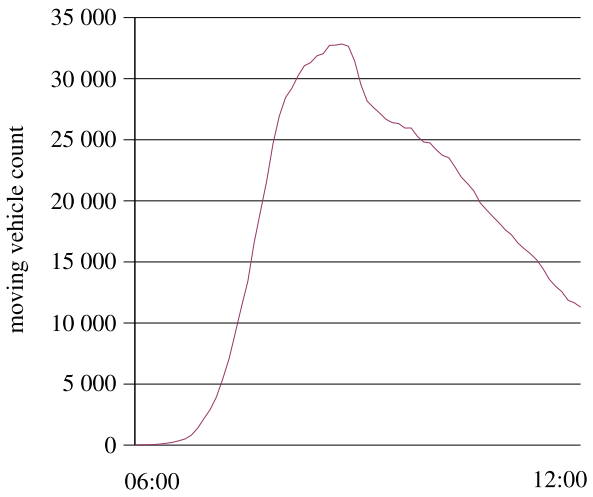

Figure 3: Simulated Berlin morning peak

A simulation of the Berlin morning peak between 6 and 12 am. The curve shows the macroscopic number of moving vehicles over time.

For the turning counter smoothing, the infinite-memory filter (8) is used. Every intersection has an individual w parameter that depend on its individual simulation time step duration T, which is location-specific in the extended cell-transmission model deployed here. For example, $\mathrm{T} = 10\,\mathrm{s}$ results in $w \approx 0.935$.

All experiments consider the morning rush hour from 6 to 12 am. Figure 3 shows the total number of moving vehicles as a function of time. More than 16 000 particles, i.e., 32 000 macroscopic vehicle units, are concurrently simulated during the rush hour peak at approximately 8:30 am.

4.1 Precision of micro/macro coupling

The microscopic particle behavior influences the macroscopic flow splits via the turning counter mechanism, whereas the microscopic particle movements are guided by the macroscopic velocity field. The precision of this micro/macro model synchronization is investigated here.

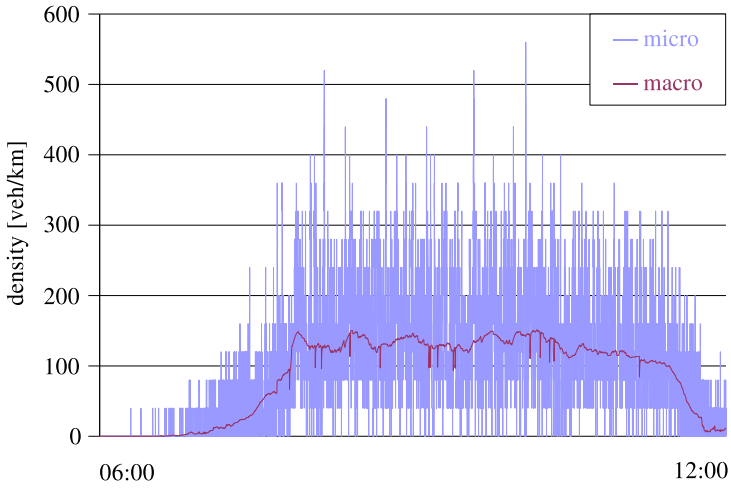

(a) Microscopic and macroscopic density trajectory for a short link of 25 m length under heavy congestion. The discrete value domain of the microscopic curve reflects the strong vehicle discretization noise. The macroscopic curve removes most of this noise. Unrealistically high microscopic densities are possible because of the massless particles. The macroscopic curve, however, is within bounds.

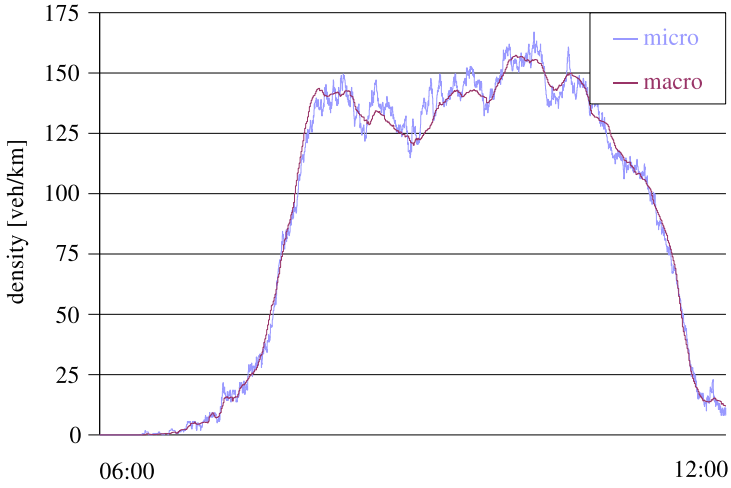

(b) Microscopic and macroscopic density trajectory for a 1.6 km long link under heavy congestion. The discretization noise has a weaker effect since a greater number of particles is averaged in the microscopic density calculations. The microscopic signal trend is tracked very well by the macroscopic curve.

Figure 4: Precision of micro/macro model synchronization

Figure 4 shows the microscopic and macroscopic traffic density trajectories for two selected links of the Berlin network. The macroscopic density is the ratio of the amount of macroscopic vehicle units on a link to the link's space capacity, which is defined as its length times its number of lanes. The microscopic density is calculated here as the quotient between twice the microscopic particle count on a link and its space capacity. The factor of two accounts for the fact that one particle represents two vehicle units in the given experimental setting.

Link (a) is only 25 meters long, whereas link (b) has a length of 1 611 meters. This difference is reflected in the much greater variance of the microscopic density on the shorter link. Both macroscopic density trajectories track the microscopic trends with high precision and almost no lag. The strong discretization noise particularly on the shorter link is significantly reduced. It is emphasized that the macroscopic trajectories are not calculated by some kind of microscopic vehicle count averaging but result implicitly from continuously tracked turning fractions that guide an appropriate amount of truly macroscopic flow across each link.

In order to avoid arbitrariness, these links were automatically chosen according to the following criteria: Link (a) exhibits the largest ratio of density to space capacity during the rush hour peak, whereas link (b) carries the largest total amount of vehicle units, i.e., the largest product of density and space capacity, in the same time interval. That is, the first criterion prefers small links, and the second criterion prefers large links. Both criteria favor congested links since uncongested conditions prevail anyway before the rush hour sets in.

A network-wide point of view is adopted by means of the following two characteristics:

$$\mathrm{MNB}(k) = \frac{100}{|A|} \sum_{a \in A} \frac{\rho_a^{\mathrm{micro}}(k) - \rho_a^{\mathrm{macro}}(k)}{\hat{\rho}} \tag{19}$$

represents the mean normalized bias where $\rho_a^{\mathrm{macro}}(k)$ ($\rho_a^{\mathrm{micro}}(k)$) is the macroscopic (microscopic) vehicle density on link a in time step k, $\hat{\rho}$ is the macroscopic jam density, and A is the set of all links in the network. The second

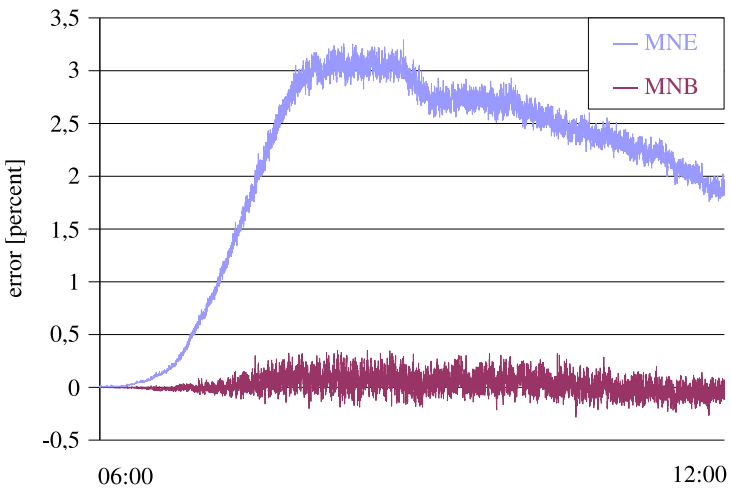

Figure 5: Mean normalized bias and error trajectories
Mean normalized bias MNB and mean normalized error MNE as defined in (19) and (20). The intermediate microscopic excess in MNB of about 1 per mille is negligible and owed to the particle entrance mechanism, which puts particles ahead of their macroscopic flow into the system. Likewise, there is a similar undershoot as the particles leave the system ahead of their macroscopic flow at the end of the rush hour.

considered characteristic is the mean normalized error

$$\mathrm{MNE}(k) = \frac{100}{|A|} \sum_{a \in A} \frac{\left| \rho_a^{\mathrm{micro}}(k) - \rho_a^{\mathrm{macro}}(k) \right|}{\hat{\rho}}. \tag{20}$$

Figure 5 shows that MNB fluctuates unsystematically around zero percent. This indicates that the mass balance between microscopic and macroscopic flow is well maintained. The maximum value of approximately three percent for MNE is moderate and plausible in consideration of Figure 4.

These results show that the micro- and the macro-model are well synchronized despite of their sparse interactions. The resulting macroscopic traffic characteristics exhibit a significantly lower discretization noise than simple averages over the microscopic particles.

4.2 Computational performance

Clearly, the computational performance of these simulations depends not only on the micro/macro coupling logic but also on the macroscopic network loading procedure. Some numbers are given here anyway to provide an intuition for the scenario size that can be handled by the proposed approach.

The computational effort for micro- and macrosimulation is distinguished in the following way. The macrosimulation runs the traffic flow model plus the turning counter tracking mechanism, which basically corresponds to repeated evaluations of (11). The microsimulation comprises the additional operations necessary to update the individual particle locations as described in Section 2.3. The total computational effort is somewhat larger than the sum of micro- and macrosimulation because of the overhead needed for bookkeeping and logical program control.

Recall that the simulated time period is 6 h = 21 600 s. To simulate this period, the macrosimulation requires 115 s and the microsimulation requires another 100 s. The complete simulation time is 240 s because of the aforementioned overhead. The resulting real time ratio of this simulation is 21 600 s / 240 s = 90. These results are obtained on a standalone 1.7 GHz Pentium 4 machine with 1 GB RAM, using the Sun Java Runtime Environment 5.0 (java, accessed 2009). Clearly, the proposed simulation scheme is applicable to large-scale scenarios. Its high performance is mainly due to the fact that the macroscopic traffic flow model only moves single-commodity flows. No care has to be taken of partial densities as it would be the case if driver behavior such as route and destination choice was represented macroscopically.

5 Summary and outlook

This article describes a computationally efficient technique for the network loading of microscopically represented travel demand with macroscopic supply models. Beyond its experimentally demonstrated compu-

tational performance, the following features of the method are noteworthy: (i) The macroscopic flow model is coupled to the microscopic demand model through a filtering mechanism that effectively removes most vehicle discretization noise. (ii) Analytical features such as continuity or differentiability of the macroscopic traffic flow model are preserved despite of the microscopic traveler representation.

These properties have already been exploited in a practically relevant application: Assuming linearizable dynamics of the macroscopic traffic flow model, it is possible to linearly predict the effect of individual–level driving decisions on the global network conditions through (11), which in turn provides information about how to adjust the demand for, e.g., system optimal assignment or demand calibration. The latter application is described in length in (Flötteröd, 2008). Another calibration–related advantage of the proposed simulation approach is the possibility to apply derivative–based calibration procedures for the identification of parameters of the macroscopic traffic flow model. Microscopic traffic flow models typically do not provide such derivatives.

The proposition of a full DTA solution procedure that exploits the proposed simulation technique is beyond the scope of this article. It is conjectured that such a procedure can be developed for a stochastic user equilibrium model where the particle population results from a Monte-Carlo evaluation of an analytical demand model that may be of great behavioral heterogeneity. The advantage of this approach would be the maintenance of a fully analytical model specification, while the microsimulation technique enters the picture merely as a numerical tool for the efficient evaluation of heterogeneous demand distributions.

References

M. Ben-Akiva, et al. (1998). 'DynaMIT: a simulation-based system for traffic prediction'. Delft, The Netherlands. DACCORD Short Term Forecasting Workshop.

M. Ben-Akiva & S. Lerman (1985). *Discrete Choice Analysis*. MIT Press series in transportation studies. The MIT Press.

J. Bowman & M. Ben-Akiva (1998). 'Activity based travel demand model systems'. In P. Marcotte & S. Nguyen (eds.), *Equilibrium and advanced transportation modelling*, pp. 27–46. Kluwer.

R. Cayford, et al. (1997). 'The NETCELL simulation package: technical description'. California PATH research report UCB-ITS-PRR-97-23, University of California, Berkeley.

N. Cetin, et al. (2003). 'A large-scale agent-based traffic microsimulation based on queue model'. In *Proceedings of the 3rd Swiss Transport Research Conference*, Monte Verita/Ascona.

C. Daganzo (1994). 'The cell transmission model: a dynamic representation of highway traffic consistent with the hydrodynamic theory'. *Transportation Research Part B* **28**(4):269–287.

C. Daganzo (1995). 'The cell transmission model, part II: network traffic'. *Transportation Research Part B* **29**(2):79–93.

A. De Palma & F. Marchal (2002). 'Real cases applications of the fully dynamic METROPOLIS tool-box: an advocacy for large-scale mesoscopic transportation systems'. *Networks and Spatial Economics* **2**:347–369.

G. Flötteröd (2008). *Traffic State Estimation with Multi-Agent Simulations*. Ph.D. thesis, Berlin Institute of Technology, Berlin, Germany.

L. Goodman (1962). 'The variance of the product of K random variables'. *Journal of the American Statistical Association* **57**(297):54–60.

M. Hilliges & W. Weidlich (1995). 'A phenomenological model for dynamic traffic flow in networks'. *Transportation Research Part B* **29**(6):407–431.

S. Hoogendoorn & P. Bovy (2001). 'State-of-the-art of vehicular traffic flow modelling'. *Proceedings of the Institution of Mechanical Engineers. Part I: Journal of Systems and Control Engineering* **215**(4):283–303.

java (accessed 2009). 'Java web site'. http://java.sun.com.

M. Jones & S. Vines (1998). 'Choosing the smoothing parameter for unordered multinomial data'. *Sociedad de Estadistica e Investigacion Operativa Test* **7**(2):411–424.

A. Kotsialos, et al. (2002). 'Traffic flow modeling of large-scale motorway networks using the macroscopic modeling tool METANET'. *IEEE Transactions on Intelligent Transportation Systems* **3**(4):282–292.

J. Lebacque (1996). 'The Godunov scheme and what it means for first order traffic flow models'. In J.-B. Lesort (ed.), *Proceedings of the 13th International Symposium on Transportation and Traffic Theory*, Lyon, France. Pergamon.

R. LeVeque (1992). *Numerical Methods for Conservation Laws*. Lectures in Mathematics: ETH Zürich. Birkhäuser.

H. S. Mahmassani (2001). 'Dynamic network traffic assignment and simulation methodology for advanced system management applications'. *Networks and Spatial Economics* **1**(3/4):267–292.

A. Mood, et al. (1974). *Introduction to the Theory of Statistics*. McGraw-Hill, New York, 3rd edition edn.

K. Nökel & M. Schmidt (2002). 'Parallel DYNEMO: meso-scopic traffic flow simulation on large networks'. *Networks and Spatial Economics* **2**(4):387–403.

S. Peeta & H. Mahmassani (1995). 'System optimal and user equilibrium time-dependent traffic assignment in congested networks'. *Annals of Operations Research* **60**:81–113.

B. Raney & K. Nagel (2006). 'An improved framework for large-scale multi-agent simulations of travel behavior'. In P. Rietveld, B. Jourquin, & K. Westin (eds.), *Towards better performing European Transportation Systems*, pp. 305–347. Routledge.

M. Rieser, et al. (2007). 'Truly agent-oriented coupling of an activity-based demand generation with a multi-agent traffic simulation'. In *Proceedings of the 86. Annual Meeting of the Transportation Research Board*, Washington, DC, USA.

K. Train (2003). *Discrete Choice Methods with Simulation*. Cambridge University Press.

P. Vovsha, et al. (2004). 'Activity-based travel forecasting models in the United States: progress since 1995 and prospects for the future'. In *Proceedings of the EIRASS Conference on Progress in Activity-Based Analysis*, Maastricht, The Netherlands.